

# Fluorescence Resonance Energy Transfer Microscopy of Localized Protein Interactions in the Living Cell Nucleus

Richard N. Day,<sup>\*,1</sup> Ammasi Periasamy,<sup>†</sup> and Fred Schaufele<sup>‡</sup>

*\*Departments of Medicine and Cell Biology, NSF Center for Biological Timing, University of Virginia Health Sciences Center, Charlottesville, Virginia, 22908; †W.M. Keck Center for Cellular Imaging, Department of Biology, University of Virginia, Charlottesville, Virginia 22904; and ‡Metabolic Research Unit and Department of Medicine, Box 0540, University of California, San Francisco, San Francisco, California 94143*

Cells respond to environmental cues by modifying protein complexes in the nucleus to produce a change in the pattern of gene expression. In this article, we review techniques that allow us to visualize these protein interactions as they occur in living cells. The cloning of genes from marine organisms that encode fluorescent proteins provides a way to tag and monitor the intracellular behavior of expressed fusion proteins. The genetic engineering of jellyfish green fluorescent protein (GFP) and the recent cloning of a sea anemone red fluorescent protein (RFP) have provided fluorescent tags that emit light at wavelengths ranging from the blue to the red spectrum. Several of these color variants can be readily distinguished by fluorescence microscopy, allowing them to be used in combination to monitor the behavior of two or more independent proteins in the same living cell. We describe the use of this approach to examine where transcription factors are assembled in the nucleus. To demonstrate that these labeled nuclear proteins are interacting, however, requires spatial resolution that exceeds the optical limit of the light microscope. This degree of spatial resolution can be achieved with the conventional light microscope using the technique of fluorescence resonance energy transfer (FRET). The application of FRET microscopy to detect the interactions between proteins labeled with the color variants of GFP and the limitations of the FRET approach are discussed. The use of different-color fluorescent proteins in combination with FRET offers the opportunity to study the complex behavior of key regulatory proteins in their natural environment within the living cell. © 2001 Academic Press

**Key Words:** fluorescence microscopy; energy transfer; transcription factors; colocalization; green fluorescent protein.

Early in the 19th century the art of light microscopy had advanced sufficiently to allow the identification of the cell as the vital unit of the living organism. Improvements in the optical instruments coupled with the development of dye chemistry soon led to the identification of the component parts of the cell, the subcellular organelles. Throughout the last half of the 20th century, both light and electron microscopes have been used to characterize the subcellular anatomy. While these studies revealed much about the ultrastructure of the subcellular organelles, these techniques provided only limited information regarding the dynamic nature of these structures.

Over the past two decades advances in molecular biology and biochemistry have provided methods to identify the individual proteins that form the component parts of the subcellular structures. *In situ* approaches that combine antibody or nucleic acid probes with the resolving power of the light or electron microscope are routinely used to demonstrate the association of specific proteins with cellular structures at the time of fixation of the cell. However, it is the dynamic interactions that occur between proteins that are the basis of life. Techniques that require either fixation of cells or disruption of cell structure can only provide correlative information regarding the relative position of proteins in the intact cell. Arguably, it is only within the context of the living cell that the consequences of the dynamic interactions between specific protein partners can be determined.

The cloning of the jellyfish green fluorescent protein (GFP) provided a protein expression tag that can be used to reveal the subcellular localization of labeled

<sup>1</sup> To whom correspondence should be addressed. Fax: (804) 982-0088. E-mail: [rnd2v@virginia.edu](mailto:rnd2v@virginia.edu).

proteins in their natural environment within the living cell. The mutagenesis of GFP has yielded proteins with different spectral properties, and some of these different-color fluorescent proteins can be used in combination to monitor the behavior of more than one protein in the same living cell. In this article we describe the methods for using fluorescence microscopy to visualize the subcellular localization of proteins tagged with the different-color fluorescent proteins. We then describe the application of fluorescence resonance energy transfer (FRET) to surpass the optical limitations of the light microscope, allowing detection of direct protein–protein interactions in the nucleus of the living cell.

## OVERVIEW OF THE FLUORESCENT PROTEINS

The green fluorescent protein (GFP) from the jellyfish *Aequoria victoria* was cloned in 1992 (1). The expression of GFP either alone or as a fusion to other proteins in a variety of cell types and in transgenic organisms has proven its utility as an *in vivo* reporter (2–10). To be fluorescent the entire protein must adopt an 11-strand  $\beta$ -barrel structure with the tripeptide (serine<sup>65</sup>–tyrosine<sup>66</sup>–glycine<sup>67</sup>) fluorophore buried in its core (reviewed in 11). The spectral properties of the *Aequoria* GFP are complex, and extensive mutagenesis of GFP has yielded fluorescent protein variants with different excitation and emission properties and enhanced fluorescence quantum yield (11–15) (see Table 1). Color variants that fluoresce from blue to yellowish green have been generated, providing several expressed-protein tags that can be readily distinguished by fluorescence microscopy. For example, changing the fluorophore serine-65 to threonine (GFP<sup>S65T</sup>) stabilized the fluorophore in a permanently ionized form with a single peak absorbance at 489 nm (13–16). The quantum yield of GFP<sup>S65T</sup> is high, and it is more resistant to photobleaching than fluorescein viewed under similar conditions (17) (see Table 1). However, photobleaching of

GFP<sup>S65T</sup> can be achieved with sufficiently intense excitation, and the approach of fluorescence recovery after photobleaching (FRAP) can be used to monitor protein trafficking in living cells. FRAP was used to measure the kinetics of GFP-labeled nuclear protein migration into a bleached area from nonbleached regions and showed that proteins can rapidly associate and dissociate with nuclear compartments (18, 19).

A second spectral variant of *Aequoria* GFP resulted when the fluorophore tyrosine-66 residue was substituted with histidine, yielding a blue shift in the emission wavelength (11, 12, 15). Even with other optimizing mutations the quantum yield of this blue fluorescent protein (BFP) is low, and it is very susceptible to photobleaching. However, because of the significant separation of its peak emission from that of other fluorescent proteins, BFP is useful in dual labeling studies (20). Moreover, its spectral overlap with the longer-wavelength fluorescent proteins, such as GFP<sup>S65T</sup>, makes BFP useful as a donor fluorophore for FRET studies (discussed below). Some of the intrinsic limitations of BFP were overcome when a cyan (blue-green) fluorescent protein (CFP) was identified (11, 12, 15). This variant resulted when the fluorophore tyrosine-66 was changed to tryptophan in combination with mutations in several other residues within the surrounding  $\beta$ -barrel structure. The peak emission for CFP is 476 nm, and it is brighter and more resistant to photobleaching than BFP (see Table 1). Further, this mutant can be combined with another color variant, the yellowish fluorescent protein (YFP) (11, 14), in two-color imaging studies and in FRET studies. The YFP variant is the most red-shifted of the mutant variants of GFP yet generated, with a peak emission at 527 nm. It also has the highest quantum yield yet achieved for the fluorescent protein variants, but it is more susceptible to photobleaching than its green counterpart (11, 21). As is discussed below, the ability to photobleach YFP can be used to an advantage in FRET studies.

The recent cloning of a red fluorescent protein (RFP)

TABLE 1  
Characteristics of the Fluorescent Proteins

Color defining GFP mutation (source)	Blue (BFP) Y66H	Cyan (CFP) Y66W	Green (GFP) S65T	Yellowish (YFP) S65G, T203Y	Red (D.s. RFP) <i>D. striata</i>
Excitation (max)	382 nm	434 nm	488 nm	514 nm	558 nm
Emission (max)	446 nm	476 nm	509 nm	527 nm	583 nm
Relative brightness ( $\epsilon \times QY$ ) <sup>a</sup>	15 <sup>b</sup>	20	70	100	100 <sup>c</sup>
Sensitivity to photobleaching	High	Low	Low	Moderate	Low <sup>c</sup>

<sup>a</sup> Relative brightness was calculated as the product of the extinction coefficient ( $\epsilon$ ) and quantum yield (QY) normalized to YFP (11, 15).

<sup>b</sup> Calculated for the P4-3 mutant (12, 15) used in these studies.

<sup>c</sup> Calculated for D.s. RFP (23).

from the Indo-Pacific sea anemone *Discosoma striata* has added yet another color to the spectrum of available fluorescent proteins (22) (see Table 1). The *D. striata* RFP is a 28-kDa protein that shares about 25% sequence identity with GFP. Because its red light emission is distinct from that of other GFPs, it has great potential as a partner in multiple labeling studies (shown below); however, the behavior of RFP when expressed *in vivo* is still under evaluation. A recent study showed the *D. striata* RFP to be a very slow maturing protein that has a strong tendency to form tetramers *in vitro* and *in vivo* (23). As with GFP and its derivatives, RFP mutagenesis experiments will likely identify RFP variants with improved spectral characteristics and behaviors for intracellular trafficking and FRET studies (23).

---

## DIGITAL IMAGING

---

When using fluorescence microscopy to detect different-color fluorophores it is important to select filter combinations that reduce the spectral "bleed-through" and optimize signal-to-noise for each fluorophore. Studies with each fluorophore alone must be done in parallel to determine if there is any significant spectral bleed-through. If there is significant bleed-through, then different filter combinations or alternative fluorophores may be required. There are many different filter combinations available from either Chroma Technology Corporation ([www.chroma.com](http://www.chroma.com)) or Omega Optical, Inc. ([www.omega-filters.com](http://www.omega-filters.com)) optimized for two- or three-color fluorescence microscopy. The selection of filter combinations to be used with the color variants of GFP is aided by examination of the published excitation and emission spectra ([www.clontech.com/gfp/excitation.html](http://www.clontech.com/gfp/excitation.html)).

For the digital imaging described here, gray-scale pictures of the fluorescence signals from each of the different-color fluorophores are acquired using a charge-coupled device (CCD) camera. The signals from the different fluorophores can be accurately quantified and compared provided that the quantum efficiency of the CCD camera is uniform over the range of light wavelengths detected. The camera used in this study has 40 to 50% quantum efficiency for light between 400 and 600 nm (Hamamatsu Orca II, <http://usa.hamamatsu.com/sys-biomedical/orcaii/orca-resp.html>). Cooling the CCD chip to decrease dark current noise and reductions in readout noise have dramatically improved the signal-to-noise ratio for CCD cameras. The field of view for these cameras, determined by the size of the CCD chip, often exceeds  $1000 \times 1000$  pixels, and the resolution, which is determined by the size of each pixel, exceeds the diffraction-limited resolution of

the light microscope. When the digitized image is read out at 12 bits, each pixel can represent up to 4096 ( $2^{12}$ ) gray levels of signal intensity.

---

## IMAGING THE SUBCELLULAR LOCALIZATION OF GFP-TAGGED PROTEINS

---

Before the GFPs, the study of protein subcellular localization in living cells relied on the use of fluorophores chemically conjugated to the cell surface or microinjected into the cells. GFPs allow the more versatile approach of detecting the subcellular location of any expressed target protein. The cDNA encoding the target protein is fused in-frame with the cDNA for GFP. The fusion cDNA is placed downstream of a suitable promoter and the transgene is then introduced into cells or transgenic organisms of interest. As with any expression tag, it is essential to verify that the fusion protein functions similarly to its endogenous counterpart by biochemical and cell physiological methods. Because GFP has no inherent localization of its own, functional GFP-fusion proteins will typically adopt the pattern of subcellular distribution of the target protein. Again, verification by immunohistochemical approaches to show the tagged protein adopts the same subcellular localization as its endogenous counterpart is essential. Once the activities of the GFP-fusion proteins have been validated, quantitative fluorescence microscopy can then be used as a noninvasive way of monitoring the subcellular localization of the fusion protein in living cells.

In this study we characterized the intranuclear location of GFP fused to the transcription factor CCAAT/Enhancer Binding Protein  $\alpha$  (C/EBP $\alpha$ ) in transiently transfected mouse 3T3 preadipocyte cells. Members of the C/EBP family of transcription factors direct programs of cell differentiation, and C/EBP $\alpha$  plays a key role in the regulation of adipocyte gene expression (24). Here, 3T3 preadipocyte cells were transfected with an expression vector encoding GFP-C/EBP $\alpha$  (see Methods). The combination of specific excitation and emission filters paired with a dichroic mirror serves to selectively excite and detect GFP fluorescence with a minimal background signal (Table 2). The excitation filter passes light at wavelengths that surrounded the peak excitation for GFP and a dichroic mirror directs the light through the objective and onto the specimen (Fig. 1A). The mirror then passes the longer-wavelength fluorescence from GFP to the emission filter, while reflecting any scattered excitation light, allowing the green light emission to reach the detector. As can be seen in Fig. 1B, the signal from GFP-C/EBP $\alpha$  was

localized exclusively to the cell nucleus. In contrast, the fluorescence from GFP when expressed alone would be diffuse throughout the cell (not shown). Moreover, Fig. 1B demonstrates that the GFP-C/EBP $\alpha$  is concentrated at specific subnuclear sites in this adipocyte cell. The endogenous C/EBP $\alpha$  had a similar pattern of subnuclear localization in differentiated mouse 3T3 cells when detected by immunohistochemical staining (24). We also observed this same pattern of subnuclear localization for GFP-C/EBP $\alpha$  in a second mouse progenitor cell line derived from the anterior pituitary, the GHFT1-5 cell line (25).

We next used three-color fluorescence microscopy to examine the subnuclear distribution of GFP-C/EBP $\alpha$  relative to two other nuclear landmarks in the living mouse pituitary cells. The GHFT1-5 cells were cotransfected with expression vectors encoding GFP-C/EBP $\alpha$  and the promyelocytic leukemia protein (PML) fused to *D.striata* RFP. The PML protein is a defining member of a group of proteins that localize to well-defined 0.5- $\mu$ m subnuclear domains called nuclear dots (26). In addition, the transfected cells were briefly treated with the cell-permeable DNA binding dye Hoechst 33342 just prior to imaging (see Methods). Digital images of the fluorescence signals from the GFP- and RFP-fusion proteins and the stained chromatin were sequentially acquired at the same focal plane using the CCD camera and the filter sets described in Table 2. The results shown in Fig. 1C demonstrate that the subnuclear distribution of GFP-C/EBP $\alpha$  paralleled the distribution of the (A-T)-rich chromatin foci that were selectively stained by the Hoechst 33342 dye. In stark contrast, the PML-RFP was localized to nuclear dots that did not overlap with the GFP-tagged C/EBP $\alpha$ . Intensity profiles generated from each of these digital images were used to precisely map the pixel-by-pixel fluorescence signals as a line of height proportional to captured

photons. The relative intranuclear distribution for each of the three fluorophores can be clearly seen in the intensity profiles shown in Fig. 1C. This type of analysis permits accurate quantification of the subnuclear localization for these fluorophores in the living cell, and is limited only by the optical resolution of the light microscope.

The resolution of the optical microscope is limited by the wavelength of visible light such that objects that are separated by less than 0.250  $\mu$ m (2500 Å) will appear to be colocalized. Thus, the observation that two proteins tagged with different-color fluorophores are colocalized *in vivo* tells us only that they are in the same vicinity, and provides little information regarding their potential to physically associate. A typical 40-kDa globular protein has a diameter of approximately 0.005  $\mu$ m (50 Å). Therefore, it would require a 50-fold improvement in optical resolution of the light microscope to visualize the physical association of proteins in the living cell. The technique of FRET microscopy provides this level of spatial resolution.

## OVERVIEW OF FRET

FRET is a quantum mechanical process involving the radiationless transfer of energy from a donor fluorophore to an appropriately positioned acceptor fluorophore. Energy can be transferred in this way only over a very limited distance, and the efficiency of energy transfer varies inversely with the sixth power of the distance separating the donor and acceptor fluorophores, effectively limiting FRET to a range of 0.002 to 0.01  $\mu$ m (27–30). Although FRET has been used for many years as a molecular ruler, it is the emergence of the fluorescent protein tags that has made FRET

TABLE 2  
Filter Combinations Used for These Studies

Fluorescent protein	Excitation filter (nm)	Dichroic mirror	Emission filter (nm)	
BFP/H33342	365/15	390	460/50	
GFP	488/20	505	535/50	
YFP	500/15	525	545/25	
RFP	535/20	570	590LP	
Donor/acceptor pair	Donor excitation filter (nm)	Dichroic mirror	Donor and acceptor emission filters	
			Donor	Acceptor
BFP/GFP	365/15	390	460/50	535/50
BFP/YFP	365/15	390	460/50	545/25

microscopy more generally applicable to biomedical research (31–40). Three basic conditions must be fulfilled for FRET to occur between a donor molecule and acceptor molecule. First, the donor emission spectrum

must significantly overlap the absorption spectrum of the acceptor. Second, the distance between the donor and acceptor fluorophores must fall within the range 0.002 to 0.01  $\mu\text{m}$ . Third, the donor and acceptor fluoro-

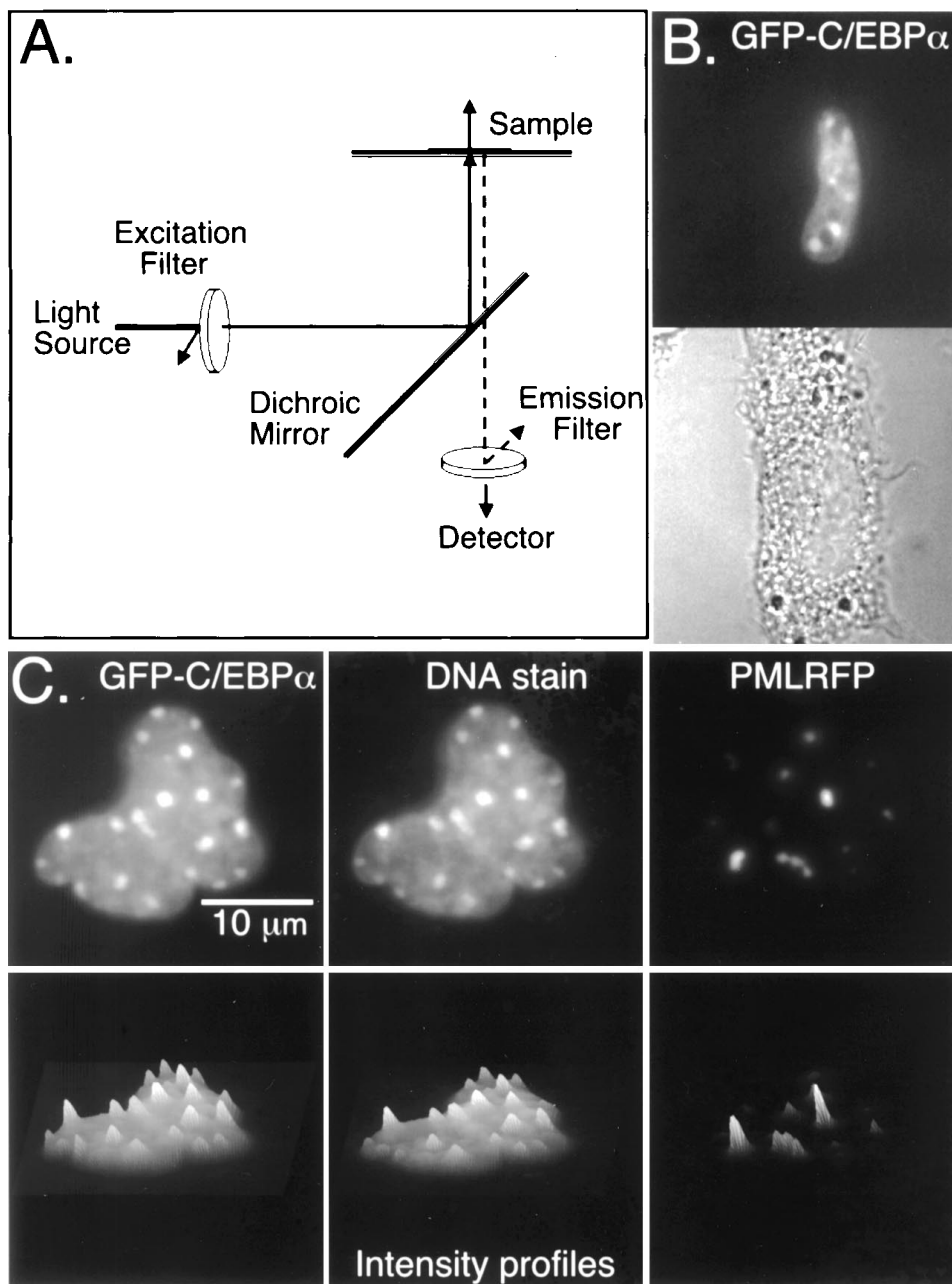


FIG. 1. Quantitative fluorescence microscopy. (A) The light pathway used for wide-field fluorescence microscopy is illustrated to show the position of the excitation and emission filters and the dichroic mirror. (B) A fluorescence image (top) and a brightfield image (bottom) of a mouse 3T3 cell expressing the GFP-C/EBP $\alpha$  fusion protein that is localized to specific intranuclear sites. (C) Fluorescence micrographs showing the nucleus of a mouse pituitary GHFT1-5 cell stained with Hoescht 33342 and coexpressing GFP-C/EBP $\alpha$  and the PML-RFP fusion protein (bar = 10  $\mu\text{m}$ ). Each image was acquired using the applicable filter sets at approximately the same gray-level intensity by varying the on-camera integration time (see Methods).

phores must be in favorable mutual orientation. The efficiency of FRET from a donor to an acceptor can be improved by increasing the overlap of the donor emission spectra with the absorption spectra for the acceptor. The trade-off for this improved efficiency, however, is that there will be an increase in the background signal resulting from spectral cross talk.

## SPECTRAL CROSS TALK

Spectral cross talk is contributed by both the donor emission that is detected in the acceptor (FRET) channel and by direct excitation of the acceptor fluorophore at the wavelength used to excite the donor. Thus, the greater the overlap in the donor–acceptor spectra, the greater the background signal from which the weak

sensitized acceptor emission must be extracted. Therefore, it is critical to determine the spectral cross talk signals for all fluorophore pairs that are to be used for FRET studies. In this study we have used the BFP variant (P4-3 variant (11, 12, 20)) as the donor fluorophore for either GFP<sup>S65T</sup> or YFP as the acceptor fluorophore. The excitation and emission spectra for the combination of BFP with GFP and YFP are shown in Fig. 2. The overlap of the BFP emission spectrum with the absorption spectrum for either GFP or YFP is adequate for FRET to occur. However, the spectral overlap for CFP emission with YFP absorption is better, which is why this combination has been frequently used in FRET studies (38–40). CFP and YFP were proven to be a suitable combination for intramolecular FRET studies, where direct tethering of CFP to YFP through a peptide linker limits the expressed donor and acceptor pair to

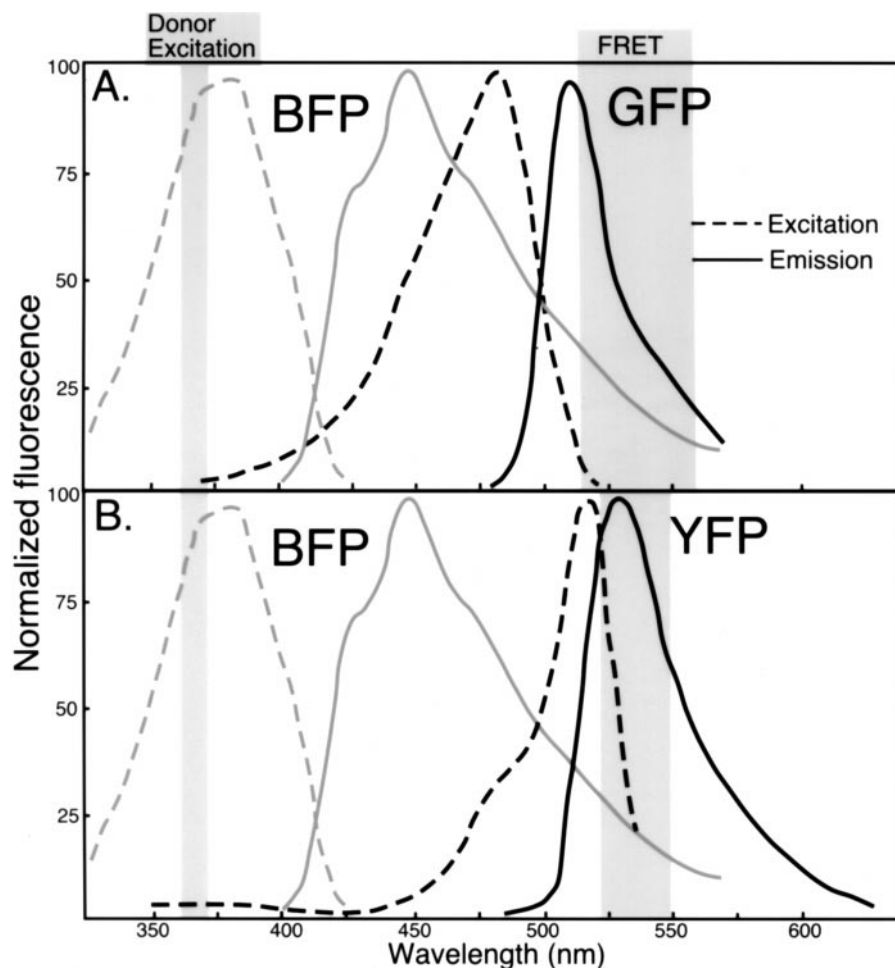


FIG. 2. Excitation and emission spectra for the BFP–GFP and BFP–YFP combinations. (A) The BFP (P4-3 variant) and GFP<sup>S65T</sup> excitation and emission spectra are shown, illustrating the overlap in BFP emission with GFP absorption, a critical requirement for FRET. (B) The overlap in BFP emission with the YFP excitation spectra. The filter sets used to detect the signals from these fluorescent protein pairs and minimize the spectral cross talk are also illustrated (gray lines).

the ratio 1:1. We find that in intermolecular FRET studies, such as those described here, where the donor-to-acceptor ratio is difficult to control, the spectral cross talk background signal for the CFP and YFP pair can be problematic. The use of BFP as the donor fluorophore, despite the drawbacks of low quantum yield and sensitivity to photobleaching (11, 15, 38), reduces the spectral cross talk background signal from which sensitized FRET signals must be detected.

The filter sets used to detect the signals from these fluorescent protein pairs, shown in Table 2, were selected to minimize the spectral cross talk and improve the signal-to-noise (S/N) ratio for the FRET signals. The donor excitation and acceptor emission channels achieved with these filter sets are also illustrated Fig. 2 (A and B). The same dichroic mirror (see Table 2) was used to acquire both the donor and acceptor (FRET) images. This is important because there can be small differences in the mechanical position of the dichroic mirror from one filter cube to another, and changing the dichroic mirror can introduce artifacts into the processed FRET images. To characterize the spectral cross talk for BFP when used in combination with either GFP or YFP, pituitary GHFT1-5 cells were transfected independently with each of the three different-color variants fused to a deletion mutant of *C/EBP $\alpha$*  (*C/EBP $\Delta$ 244*). Like wild-type *C/EBP $\alpha$* , the tagged deletion mutant was localized to foci in the nucleus of the transfected GHFT1-5 cells (see Fig. 3). The transfected cells were grown overnight on glass coverslips and then digital images of the cell nuclei were acquired using the filter sets described in Table 2 (see Methods). Each of the fluorophore-specific images was collected at similar gray level intensities, and identical conditions were then used to acquire images using the FRET filter set. This allowed the measurement of the donor and acceptor spectral cross talk background signals in the FRET channel. To simplify this comparison, histograms showing the pixel distribution for each set of images were then plotted. The histograms in Fig. 3A show the component of BFP emission that is detected in the FRET channel (top panel). The lower panel of Fig. 3A shows GFP emission that occurs as the result of the 365-nm donor excitation light (bottom panel). Similar images of cells expressing either BFP or YFP, shown in Fig. 3B, demonstrate the two components of spectral cross talk contributing to the background signal in the FRET channel for this pair. The spectral cross talk is reduced when using YFP because of its red-shifted excitation spectrum (Fig. 2) and the narrower FRET emission filter (Table 2). These results show the background signal from which sensitized acceptor emission must be extracted.

---

## FRET IMAGING

---

When donor- and acceptor-tagged proteins are coexpressed, the detection of sensitized acceptor fluorescence at the excitation wavelength for the donor (FRET) indicates the distance separating the tagged protein partners is between 0.002 and 0.01  $\mu\text{m}$ . Here, we demonstrate the acquisition of FRET signals from living cells coexpressing BFP- and GFP-*C/EBP $\Delta$ 244*. When coexpressed, the GFP- and BFP-*C/EBP $\Delta$ 244* were localized in foci in the nucleus of the transfected GHFT1-5 cells (see Fig. 4). The *C/EBP $\alpha$*  protein is a basic region-leucine zipper (b-zip) transcription factor that binds to DNA via the basic region as dimers involving the leucine zipper. Our studies indicate that the b-zip region of *C/EBP $\alpha$*  (AA 244-358) is both necessary and sufficient for the subnuclear targeting to the chromatin foci described above (data not shown, see Fig. 1C). If the labeled *C/EBP $\Delta$ 244* proteins are interacting in these subnuclear sites such that the fluorophores are separated by less than 0.01  $\mu\text{m}$ , then FRET microscopy can reveal these interactions. Note that if the GFP- and BFP-*C/EBP $\Delta$ 244* are dimerized, only 50% of the complexes will be productive donor (BFP)- and acceptor (GFP)-tagged pairs, with the remainder being nonproductive BFP-BFP and GFP-GFP complexes.

A reference image is acquired using the GFP filter set to establish the expression level for GFP-*C/EBP $\Delta$ 244* in the chosen cell (Fig. 4A). A digital image of the donor signal from BFP-*C/EBP $\Delta$ 244* was then obtained (Fig. 4B), followed by acquisition of the acceptor (FRET) image using identical conditions and changing only the emission filter (Fig. 4C). The histograms shown in Fig. 4 demonstrate that the signal in the FRET channel exceeds the donor signal, and is greater than the signal expected for spectral cross talk alone (see Fig. 3A). This FRET signal, however, still contains the spectral cross talk components contributed by both the donor and acceptor. Mathematical approaches to correct for the spectral cross talk component and then extract the FRET signal can provide a more quantitative method for measuring FRET (33, 41). This approach requires that data sets be obtained from cells expressing donor or acceptor alone, with each set being acquired under the same conditions used for the FRET measurements. These data sets can then be used to derive coefficients to correct for spectral cross talk. The precise and reproducible measurement of those correction coefficients is essential to avoid the introduction of errors in data processing

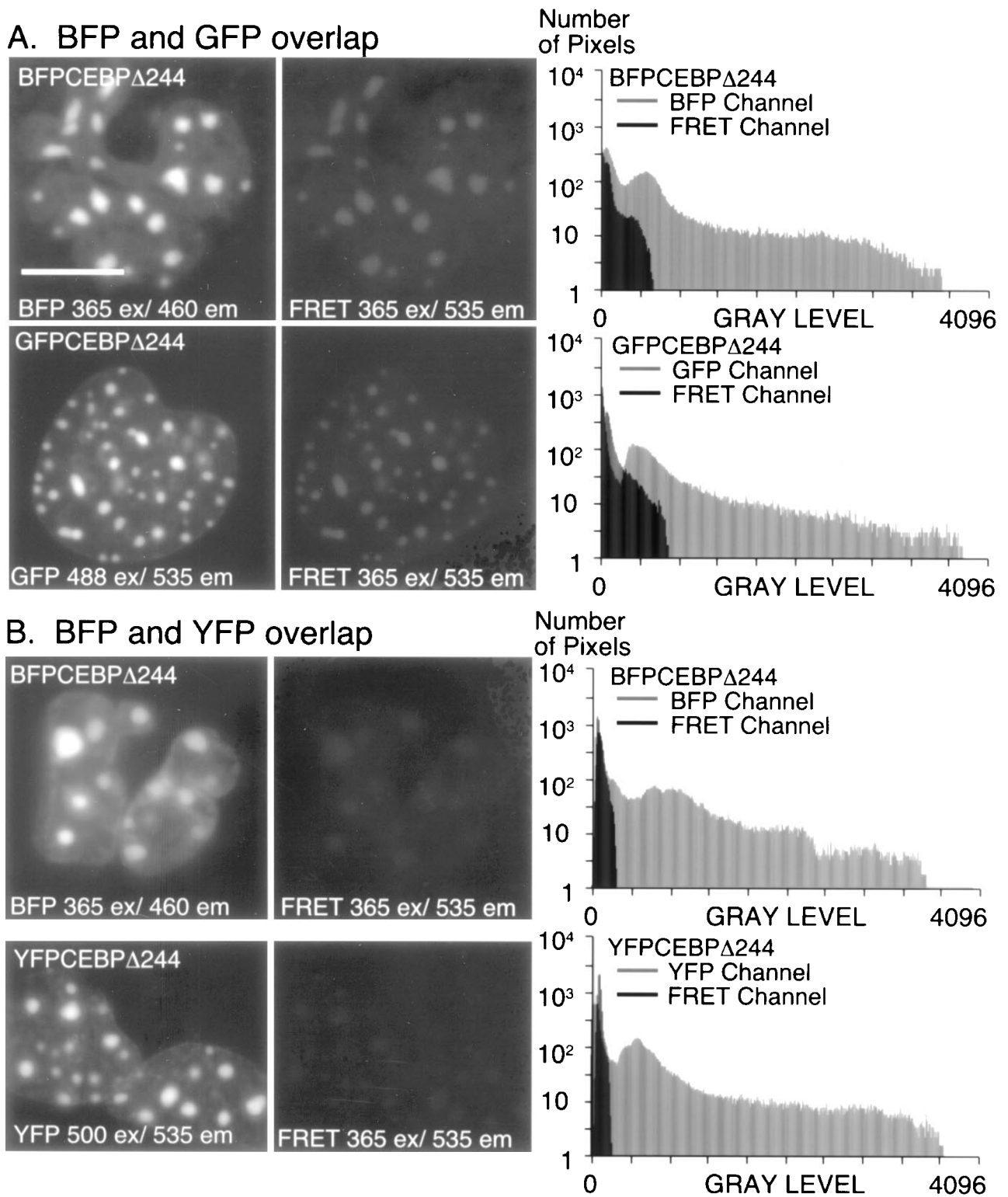


FIG. 3. Spectral cross talk. The spectral cross talk for the (A) BFP–GFPS65T and (B) BFP–YFP combinations was determined. Pituitary GHFT1-5 cells were transfected independently with BFP-, GFP-, or YFP-C/EBP $\Delta$ 244. Digital images of the nuclei of cells expressing each fusion protein were then acquired using the filter sets described in Table 2 (see Methods) (bar = 10  $\mu$ m). In each case the fluorophore-specific images and the images acquired with the FRET filter set were obtained under identical conditions, allowing direct comparison of the spectral cross talk signal in the FRET channel. Histograms are plotted to show the pixel distribution for each set of images demonstrating the BFP emission detected in the FRET channel (top panels A, B). The lower panels show the GFP (A) and YFP (B) emission that occurs as the result of the 365-nm donor excitation light.

(42). A second approach, demonstrated below, uses acceptor photobleaching to remove the acceptor fluorophore, and then measures the effect of the loss of acceptor on the donor fluorescence intensity.

## FRET AND ACCEPTOR PHOTOBLEACHING

When sensitized FRET emission occurs there is a concomitant quenching of the donor fluorescence signal

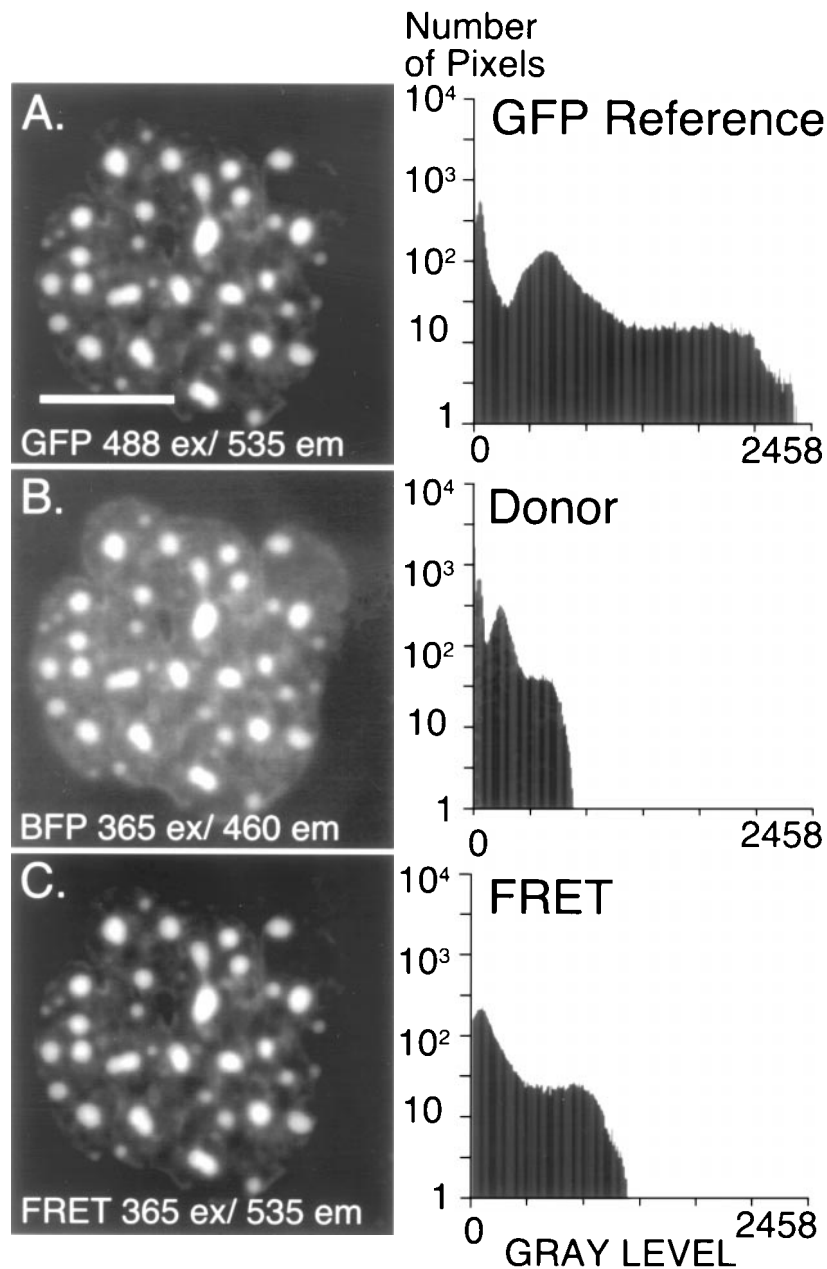


FIG. 4. FRET microscopy with BFP and GFP. Pituitary GHFT1-5 cells were cotransfected with expression vectors encoding GFP- and BFP-C/EBP $\Delta$ 244. (A) A reference image showing the nucleus of a cell coexpressing these two proteins was acquired using the GFP filter set to establish the expression level for GFP-C/EBP $\Delta$ 244 (bar = 10  $\mu$ m). (B) A second digital image was obtained at the same focal plane using the donor filter set to detect the BFP-C/EBP $\Delta$ 244 signal. (C) By changing only the emission filter and using identical conditions as for (B), the acceptor (FRET) image was then acquired. The histograms shown demonstrate that the signal in the FRET channel exceeds the donor signal, and is greater than the signal expected for spectral cross talk alone (see Fig. 3A).

because some of the donor excitation energy is being transferred directly to the acceptor. Ideally, both quenching of the donor signal and the sensitized acceptor emission should be measured to confirm that FRET has occurred, and the technique of acceptor photobleaching provides a method for making both measurements (42, 43). The selective photobleaching of the acceptor fluorophore abolishes FRET, and in the regions of the cell where FRET occurred, there will be an enhancement in the donor emission because of dequenching. The YFP variant is sensitive to photobleaching (21, 42) (see Table 1), making it an ideal candidate for confirmation of FRET by acceptor photobleaching. When coexpressed in GHFT1-5 cells, YFP- and BFP-C/EBP $\Delta$ 244 were localized in foci in the cell nuclei (see Fig. 5). As was done in the previous experiment (Fig. 4), a reference image showing YFP expression was acquired (Acceptor 1, Fig. 5A, left). Images of acceptor emission with donor excitation (FRET 1, Fig. 5B, left) and the donor emission (Donor 1, Fig. 5C, left) were then obtained by changing only the emission filter.

The YFP acceptor was then photobleached by exposure to 500-nm light (Acceptor 2, Fig. 5A, see Methods). This selective acceptor photobleaching reduced the signal in the FRET channel to the donor bleed-through component alone (FRET 2, Fig. 5B). In contrast, the donor fluorescence intensity increased after acceptor photobleaching because of dequenching (Donor 2, Fig. 5C; compare histograms of fluorescence intensity before and after photobleaching). The recovery of donor from quenching can be quantified by subtracting the Donor 1 digital image from the Donor 2 image (Fig. 5D, left), and the subnuclear location of the dequenched donor signal, which is where FRET was occurring, can be precisely mapped in the intensity profile (Fig. 5D, right). Together, the demonstration of a FRET signal above the expected spectral cross talk background and the demonstration of increased donor signal after acceptor photobleaching provide strong evidence for dimerization of these proteins at discrete subnuclear sites in these living cells. The challenge now is to use this approach to provide new insight into the assembly of these nuclear factors.

## METHODS

There are many different methods available for the transient expression of GFP-fusion proteins in living cells. The efficiency of these different methods can be very dependent on the cell type being used. For the studies described here, we have used electroporation of mouse pituitary GHFT1-5 cells, and typically found

that approximately 40% of the cells expressed the fusion proteins as determined by fluorescence microscopy. The ideal cells for imaging are large with a very flat morphology that can be grown on coverglass. The cells can be encouraged to attach to glass by treating the glass with poly(L-lysine), collagen, or other matrices.

### Transfection by Electroporation

1. Mix the plasmid vectors encoding the fusion proteins in sterile electroporation cuvettes and use empty vector DNA to keep the total amount of DNA constant for a given experiment. The amount of DNA per cuvette typically ranges from 5 to 30  $\mu$ g and optimal concentrations must be determined by experimentation. Both 0.2- and 0.4-cm-gap cuvettes are available, and electroporation conditions must be optimized for each cell line.

2. Rinse the cell monolayer with phosphate-buffered saline, and then briefly treat the cells with trypsin (0.05%) in 0.53 mM EDTA. Remove the trypsin-EDTA solution.

3. When cells begin to release from the surface of the flask, recover the cells in culture medium containing serum. Wash the cells two times by centrifugation in Dulbecco's calcium/magnesium-free phosphate-buffered saline.

4. Resuspend the cells to a final concentration of approximately  $1 \times 10^7$  cells/ml in Dulbecco's calcium/magnesium-free phosphate-buffered saline. Add 400  $\mu$ l of the cell suspension to each 0.2-cm-gap electroporation cuvette containing the DNA.

5. Gently mix the contents of the cuvette and then pulse the cells at the desired voltage and capacitance. The optimal electroporation conditions for each different cell type must be determined empirically. For a 400- $\mu$ l suspension of GHFT1-5 cells in 0.2-cm-gap cuvettes, we use a 220-V pulse at a total capacitance of 1200  $\mu$ F. The typical pulse durations obtained under these conditions are 9–10 ms.

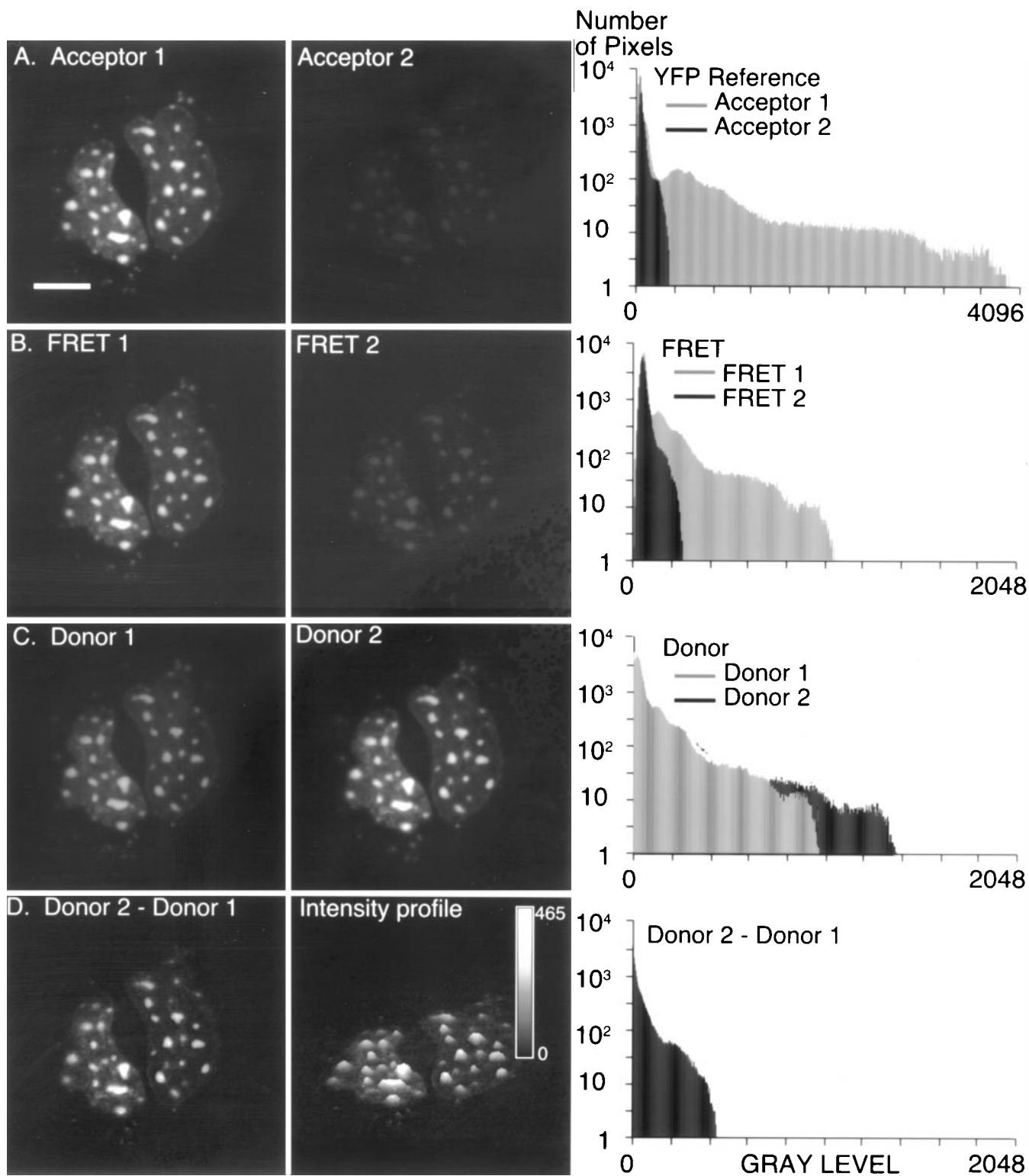
6. Immediately recover the cells from the cuvette and dilute in phenol red-free tissue culture medium containing serum.

7. Inoculate the cells dropwise onto a sterile coverglass in 35-mm culture dishes. Allow the cells to attach to the coverglass for approximately 20 min prior to gently flooding the culture dish with medium.

8. Place the cultures in an incubator for 18 to 36 h prior to imaging.

### Quantitative Fluorescence Microscopy using GFP, RFP, and Hoechst 33342

The use of high-quality apochromatic optics, high-numerical-aperture water-immersion objectives, and



uniform specimen illumination will greatly improve the sensitivity and resolution of images obtained from living cell preparations. The imaging system used for the present study consisted of an inverted microscope equipped for both epifluorescence and transmitted illumination (IX-70, Olympus America Inc., Melville, NY). For living specimens water-immersion lenses provide better resolution deeper into the optical section because they reduce spherical aberration, and a 1.2-numerical-aperture 60 $\times$  aqueous-immersion objective lens was used here. For excitation of several different fluorophores, uniformity across the spectrum is an important characteristic of the excitation source, and our light source was a 100-W mercury–xenon arc lamp. The excitation filter and emission filter wheels and the neutral density (ND) filter wheel (Ludl Electronic Products Ltd., Hawthorne, NY) were interfaced with a Silicon Graphics, Inc. (SGI) computer system. The dichroic mirrors were installed in filter cubes. The detector used was a Hamamatsu Orca II cooled CCD camera (Hamamatsu, Bridgewater, NJ). The SGI-based Isee software (Inovision Corp., Raleigh, NC) was used to integrate the operation of the filter wheels, to control the camera, and to store and process the acquired images.

1. Place the coverglass with the monolayer of transfected cells in a suitable chamber that fits the stage of the microscope. For chambers where the culture is exposed to room air, it is important to use a culture medium buffered to maintain pH in room air.

2. For DNA staining in living cells, we used Hoechst 33342 (Molecular Probes, Eugene, OR) added to a final concentration of 0.5  $\mu\text{g}/\text{ml}$  for approximately 20 min prior to imaging.

3. Because of its photostability, we first scan the field of cells for GFP expression. Temporary images of healthy cells that are expressing detectable levels of the GFP-fusion protein are obtained to allow adjustment of the focus and camera integration time. It is important to use the full dynamic range of the camera (up to 4096 gray levels for a readout at 12 bits), but it is critical that there be no saturated pixels in the final image, since signal level cannot be determined in this situa-

tion. The final image is then acquired and saved for processing using the applicable computer software. Acquiring a bright-field image of the selected cells is useful for the demonstration of the subcellular localization of the expressed protein (Fig. 1B).

4. Sequential images of the different fluorophores are obtained at the same focal plane by switching the excitation and emission filter wheels and manually switching the dichroic filter cubes. The camera integration time was adjusted to obtain an optimal image, and the final image was saved for further processing. This process was then repeated for the blue Hoechst 33342 dye.

5. The acquired images can then be background subtracted using computer software, followed by generation of intensity profiles and conversion to TIFF file format. For this study we used the Inovision ISEE computer software (Inovision Corp., Raleigh, NC), and the TIFF images were processed for presentation using Canvas 7.0 (Denaba Systems, Inc., Miami, FL) and printed at 300 dots per inch using a Codonics NP 1600 dye diffusion printer (Codonics, Inc., Middleburg Heights, OH).

### FRET Microscopy

The conventional inverted fluorescence microscope described above was also used for FRET imaging (reviewed in 34). Because of the sensitivity of BFP to photobleaching it is important to scan and acquire images of cells expressing the GFP or YFP partners first before acquiring the donor image. Using transient cotransfection of expression vectors described above we found good agreement in the expression levels for both donor and acceptor fusion proteins. Therefore, scanning the field for cells expressing a certain level of green fluorescence is often a good predictor of the BFP expression level in that cell and, importantly, avoids photobleaching of the BFP. It is important to achieve protein expression levels that will allow the use of some neutral density filtration. This will reduce the spectral scattering from the excitation light source and help to control the photobleaching BFP.

FIG. 5. FRET microscopy and acceptor photobleaching with BFP and YFP. The selective photobleaching of the acceptor fluorophore abolishes FRET, and enhances donor emission because of dequenching. (A, left) The reference image showing the nuclei of two adjacent cells coexpressing YFP– and BFP–C/EBP $\Delta$ 244 (Acceptor 1) (bar = 10  $\mu\text{m}$ ). (B, left) Images of acceptor emission with donor excitation (FRET 1) and (C, left) the BFP–C/EBP $\Delta$ 244 emission (Donor 1) were then obtained under identical conditions by changing only the emission filter. (A, right) The YFP acceptor was then photobleached by exposure to 500-nm light (see Methods); a second reference image (Acceptor 2) was obtained using the same conditions as for the first image. (B, right) The effect of selective acceptor photobleaching on the FRET signal (FRET 2) and (C, right) the donor fluorescence intensity (Donor 2) is shown. (D, left) The dequenching of the donor was quantified by subtracting the Donor 1 digital image from the Donor 2 image (D, right), and the subnuclear location where FRET occurred was mapped in the intensity profile; the calibration bar indicates the gray-level intensity.

1. As described above for colocalization studies, scan the field of cells to find healthy cells that are expressing reasonable levels of the acceptor fusion protein.

2. Acquire and save the acceptor fluorescence image. This provides a reference image for the acceptor expression and for the comparison with the acceptor spectral cross talk component.

3. With the excitation shutter closed, switch to the BFP filter set and the donor/FRET dichroic mirror and acquire the donor image at the same focal plane as the reference image. Save the image for processing.

4. Switch to the acceptor (FRET) emission filter and collect the FRET image using the *identical* conditions and integration time used for the donor image.

5. For photobleaching of the YFP acceptor, we have used approximately 5-min exposure of the specimen to unfiltered 500-nm excitation light. This typically reduces the YFP fluorescence signal more than five fold. Acquire a second acceptor reference image to document photobleaching.

6. Acquire a second donor image at the same focal plane as the first, using the BFP filter set and the donor/FRET dichroic mirror.

7. Acquire a second FRET image to document the reduction in the FRET signal resulting from acceptor photobleaching.

8. The images are then processed by background subtraction of the acceptor reference, donor and FRET images. Images before and after acceptor photobleaching can be combined in a single mosaic image for the direct comparison of signal level. The digital image of the donor before acceptor photobleaching can also be subtracted from donor after bleaching to demonstrate donor dequenching. An intensity profile map of the donor 2-donor 1 image can be used to represent the change in donor signal, or the images can be combined into a single mosaic image and a lookup table can be applied to indicate the pixel-by-pixel fluorescence signal intensity in the side-by-side images. For direct comparison, histograms of the signal levels can be plotted for both donor 1 and donor 2 fluorescence.

9. The comparison of these results with those from the control experiments described above will demonstrate if FRET emission has occurred, providing evidence for protein-protein interactions. It is critical that the control and the experimental images are acquired under the same conditions since FRET must be quantified against the fluorescence separately emitted from the donor and acceptor in the FRET channel. The levels of control protein expression should be as similar as possible to those acquired under the experimental conditions.

---

## LIMITATIONS AND CAUTIONS FOR FRET MICROSCOPY

---

The failure to detect FRET from a pair of labeled proteins carries no intrinsic information regarding the association of the proteins. There are many potential reasons for interacting protein partners to fail to produce FRET signals. Because the detection of weak FRET signals is critically dependent on the efficiency of FRET, it is important to optimize this by choosing the donor fluorophore with an emission spectrum that has a significant overlap with the absorption of acceptor. Since FRET will be most efficient when the stoichiometry favors that proteins fused to the donor fluorophore are preferentially interacting with proteins fused to the acceptor, one can also increase the concentration of the acceptor protein relative to the donor protein. It is important to realize that the endogenous protein partners for the donor and acceptor proteins will interact and compete for potential productive interactions. The cells used in the studies presented here were selected because they are devoid of endogenous C/EBP $\alpha$  (44). As with any approach involving the expression of proteins in living cells, artifacts that arise from overexpression of the fusion proteins are a concern. Control experiments with labeled proteins that colocalize, but that should not physically interact, can be used to assess the contribution of nonspecific interactions to measured FRET signals. Finally, FRET measurements are limited by the accuracy of quantifying fluorescence intensity, which is more prone to artifacts at weaker energy transfer signals. It is therefore essential to characterize your individual equipment for the intensity limits below which fluorescence quantification becomes insufficiently rigorous for accurate FRET determination. In such circumstances of weak FRET, fluorescence lifetime imaging of the donor fluorophore (see below) may offer a significant improvement in sensitivity for determining the physical interactions between molecules in living cells.

---

## CONCLUSIONS AND FUTURE DIRECTIONS

---

We have reviewed the technique of FRET microscopy for studying protein-protein interactions in the nucleus of the living cell. We outlined some of the important considerations in using the different-color variants of the fluorescent proteins in multicolor fluorescence microscopy and for detecting FRET. Finally, we demonstrated how acceptor photobleaching could improve the resolution of localized FRET signals within the cell. Factors that limit the detection of the weak fluorescent

signals associated with FRET include the contribution of autofluorescence, photobleaching, and light scattering to the image background. These factors can be especially significant for the acquisition of images using BFP. These latter two limitations can be overcome by detecting FRET through its effect on the fluorescence lifetime of the donor fluorophore. The average lifetime of a fluorescent molecule in the excited state is typically less than 10 ns, and the lifetime is critically dependent on the local environment surrounding the probes (45, 46). The fluorescence lifetime imaging (FLIM) technique detects the nanosecond decay kinetics of the fluorophores, providing a spatial lifetime map of these probes within the cell. FRET from a donor fluorophore to acceptor molecules in the local environment substantially influences the donor fluorescence lifetime. An important advantage of combining the FRET and FLIM imaging modalities is that only the donor emission lifetimes need to be monitored to detect interactions between the labeled proteins. The technique is blind to the acceptor emission, and only those acceptor molecules close enough to receive donor excited state energy are detected. Moreover, when used in the multiphoton excitation mode, fluorescence lifetime imaging microscopy offers a potential improvement over standard epifluorescence microscopy in monitoring dynamic protein-protein interactions between GFP-fusion proteins. Two-photon excitation of a donor fluorophore using femtosecond pulsed laser light limits the excitation to the focal volume, thus minimizing photobleaching of the donor probe and reducing the absorbance and light scattering from the sample.

## ACKNOWLEDGMENTS

We thank Cindy Booker for expert assistance and Bill Hyun of the UCSF Cancer Center for microscopy advice. This work was supported by Grant NIH DK47301 and the NSF Center for Biological Timing (R.N.D.), and by American Cancer Society Grant RPG-94-028-TBE and the UCSF Academic Senate Committee on Research (F.S.).

## REFERENCES

- Prasher, D. C., Eckenrode, V. K., Ward, W. W., Prendergast, F. G., and Cormier, M. J. (1992) *Gene* 111, 229–233.
- Chalfie, M., Tu, Y., Euskirchen, G., Ward, W. W., and Prasher, D. C. (1994) *Science* 263, 802–805.
- Cubitt, A. B., Heim, R., Adams, S. R., Boyd, A. E., Gross, L. A., and Tsien, R. Y. (1995) *Trends Biochem. Sci.* 20, 448–455.
- Gerdes, H. H., and Kaether, C. (1996) *FEBS Lett.* 389, 44–47.
- Plautz, J. D., Day, R. N., Dailey, G. M., Welsh, S. B., Hall, J. C., Halpain, S., and Kay, S. A. (1996) *Gene* 173, 83–87.
- Zhuo, L., Sun, B., Zhang, C. L., Fine, A., Chiu, S. Y., and Messing, A. (1997) *Dev. Biol.* 187, 36–42.
- Take-Uchi, M., Kawakami, M., Ishihara, T., Amano, T., Kondo, K., and Katsura, I. (1998) *Proc. Natl. Acad. Sci. USA* 95, 11775–11780.
- Fleischmann, M., Bloch, W., Kolossov, E., Andressen, C., Muller, M., Brem, G., Hescheler, J., Addicks, K., and Fleischmann, B. K. (1999) *FEBS Lett.* 440, 370–376.
- Sun, B., Xu, P., and Salvaterra, P. M. (1999) *Proc. Natl. Acad. Sci. USA* 96, 10438–10443.
- Xian, M., Honbo, N., Zhang, J., Liew, C. C., Karliner, J. S., and Lau, Y. F. (1999) *J. Mol. Cell Cardiol.* 31, 2155–2165.
- Tsien, R. Y. (1998) *Annu. Rev. Biochem.* 67, 509–544.
- Heim, R., and Tsien, R. Y. (1996) *Curr. Biol.* 6, 178–182.
- Heim, R., Prasher, D. C., and Tsien, R. Y. (1994) *Proc. Natl. Acad. Sci. USA* 91, 12501–12504.
- Heim, R., Cubitt, A. B., and Tsien, R. Y. (1995) *Nature* 373, 663–664.
- Cubitt, A. B., Woollenweber, L. A., and Heim, R. (1999) *Methods Cell Biol.* 58, 19–30.
- Brejč, K., Sixma, T. K., Kitts, P. A., Kain, S. R., Tsien, R. Y., Ormo, M., and Remington, S. J. (1997) *Proc. Natl. Acad. Sci. USA* 94, 2306–2311.
- Patterson, G. H., Knobel, S. M., Sharif, W. D., Kain, S. R., and Piston, D. W. (1997) *Biophys. J.* 73, 2782–2790.
- McNally, J. G., Muller, W. G., Walker, D., Wolford, R., and Hager, G. L. (2000) *Science* 287, 1262–1265.
- Phair, R. D., and Misteli, T. (2000) *Nature* 404, 604–609.
- Day, R. N., Nordeen, S. K., and Wan, Y. (1999) *Mol. Endocrinol.* 13, 517–526.
- Ellenberg, J., Lippincott-Schwartz, J., and Presley, J. F. (1998) *Biotechniques* 25, 838–842.
- Matz, M. V., Fradkov, A. F., Labas, Y. A., Savitsky, A. P., Zaraisky, A. G., Markelov, M. L., and Lukyanov, S. A. (1999) *Nat. Biotechnol.* 17, 969–973.
- Baird, G. S., Zacharias, D. A., and Tsien, R. Y. (2000) *Proc. Natl. Acad. Sci. USA* 97, 11984–11989.
- Tang, Q. Q., and Lane, M. D. (1999) *Genes Dev.* 13, 2231–2241.
- Lew, D., Brady, H., Klausning, K., Yaginuma, K., Theill, L. E., Stauber, C., Karin, M., and Mellon, P. L. (1992) *Genes Dev.* 7, 683–693.
- Sternsdorf, T., Grotzinger, T., Jensen, K., and Will, H. (1997) *Immunobiology* 198, 307–331.
- Förster, T. (1965) in *Modern Quantum Chemistry* (Sinanoglu, O., Ed.), Vol. 3, pp. 93–137, Academic Press, New York.
- Stryer, L. (1978) *Annu. Rev. Biochem.* 47, 819–846.
- Jovin, T. M., and Arndt-Jovin, D. J. (1989) in *Cell Structure and Function by Microspectrofluorometry* (Kohen, E., and Hirschberg, J. G., Eds.), pp. 99–117, Academic Press, San Diego.
- Wu, P., and Brand, L. (1994) *Anal. Biochem.* 218, 1–13.
- Mitra, R. D., Silva, C. M., and Youvan, D. C. (1996) *Gene* 173, 13–17.
- Day, R. N. (1998) *Mol. Endocrinol.* 12, 1410–1419.
- Mahajan, N. P., Linder, K., Berry, G., Gordon, G. W., Heim, R., and Herman, B. (1998) *Nat. Biotechnol.* 16, 547–552.
- Periasamy, A., and Day, R. N. (1999) *Methods Cell Biol.* 58, 293–314.
- Pollok, B. A., and Heim, R. (1999) *Trends Cell Biol.* 9, 57–60.
- Llopis, J., Westin, S., Ricote, M., Wang, Z., Cho, C. Y., Kurokawa, R., Mullen, T. M., Rose, D. W., Rosenfeld, M. G., Tsien, R. Y., Glass, C. K., and Wang, J. (2000) *Proc. Natl. Acad. Sci. USA* 97, 4363–4368.
- Kraynov, V. S., Chamberlain, C., Bokoch, G. M., Schwartz, M. A., Slabaugh, S., and Hahn, K. M. (2000) *Science* 290, 333–337.

38. Miyawaki, A., Llopis, J., Heim, R., McCaffery, J. M., Adams, J. A., Ikura, M., and Tsien, R. Y. (1997) *Nature* 388, 882–887.
39. Miyawaki, A., Griesbeck, O., Heim, R., and Tsien, R. Y. (1999) *Proc. Natl. Acad. Sci. USA* 96, 2135–2140.
40. Damelin, M., and Silver, P. A. (2000) *Mol. Cell* 5, 133–140.
41. Gordon, G. W., Berry, G., Liang, X. H., Levine, B., and Herman, B. (1998) *Biophys. J.* 74, 2702–2713.
42. Miyawaki, A., and Tsien, R. Y. (2000) *Methods Enzymol.* 327, 472–500.
43. Wouters, F. S., Bastiaens, P. I., Wirtz, K. W., and Jovin, T. M. (1998) *EMBO J.* 17, 7179–7189.
44. Schaufele, F. (1996) *J. Biol. Chem.* 271, 21484–21489.
45. Gadella, T. W., Jr., and Jovin, T. M. (1995) *J. Cell Biol.* 29, 1543–1558.
46. Bastiaens, P. I., and Squire, A. (1999) *Trends Cell Biol.* 9, 48–52.